Journal of Machine Construction and Maintenance
QUARTERLY ISSN 1232-9312 4/2018(111)

p. 47–55

Sergiy LAVRYNENKO[a], Mirosław RUCKI[b,*], Zbigniew SIEMIĄTKOWSKI[b],
Wojciech KUCHARCZYK[b], Dmitrij MOROZOW[b], Mykola ZAPOLOVSKY[a], Oleg LAVRYNENKO[a]
[a] National Technical University "Kharkov Polytechnic Institute", Ukraine
[b] Faculty of Mechanical Engineering, Kazimierz Pulaski University of Technology and Humanities in Radom, Poland
[*] Corresponding author: m.rucki@uthrad.pl

IMPACT OF MACHINING CONDITIONS ON EXPLOITAION STABILITY OF THERMOPLASTIC COMPOSITE SCINTILLATORS

Key words: scintillator, polystyrene, fine milling, surface topography, degradation.

Abstract: The paper presents research results on the degradation of scintillators made out of thermoplastic composite materials based on polystyrene (PS). The samples were machined with the tools made out of three different material types: refractory alloys, synthetic diamonds, and diamonds mined from the Earth. The investigations enabled us to establish relations between the polystyrene scintillators' machining conditions and the final roughness of their surface, as well as the impact of the surface quality on their optical stability. It was found that optimal feed of the preliminary machining was no more than 0.1 mm/tooth, and, for profiling or finishing milling, the rate was ca. 0.02 to 0.04 mm/tooth. Both an increase and decrease of the finishing milling parameters worsened the quality of the surface. It was proved that the optical elements can keep unchanged their characteristics during exploitation as long as 10 years if certain machining conditions are kept. The result can be attributed to high surface integrity in terms of surface microcracks, edge micro-damages, and inner stresses.

Wpływ warunków obróbki na stabilność eksploatacyjną scyntylatorów wykonanych z kompozytów termoplastycznych

Słowa kluczowe: scyntylator, polistyren, frezowanie precyzyjne, topografia powierzchni, degradacja materiału.

Streszczenie: W artykule przedstawiono wyniki badań nad degradacją materiału scyntylatorów wykonanych z termoplastycznych kompozytów na bazie polistyrenu (PS). Badane próbki obrabiano narzędziami z różnych materiałów: ze stopów trudnotopliwych, z diamentów sztucznych oraz z diamentów naturalnych. Na podstawie wyników ustalono zależności pomiędzy warunkami obróbki scyntylatorów polistyrenowych a wynikową topografią powierzchni, a następnie pomiędzy jakością powierzchni a stabilnością optyczną scyntylatorów. Ustalono, że optymalny posów dla obróbki zgrubnej wynosił nie więcej niż 0,1 mm/ostrze, zaś dla dokładnej i wykańczającej ok. 0,02÷0,04 mm/ostrze. Zarówno zwiększenie, jak i zmniejszenie tych wielkości pogarszało jakość powierzchni. Stwierdzono, że zachowanie określonych parametrów obróbki powoduje, iż elementy optyczne mogą zachowywać swoje właściwości eksploatacyjne nawet do 10 lat, prawdopodobnie ze względu na uzyskany wysoki stopień integracji powierzchni i minimalizację mikropęknięć, mikrouszkodzeń krawędzi oraz naprężeń wewnętrznych.

Introduction

Organic plastic scintillators were described as early as the 1960s [1]. The transparent composite scintillators may be produced when inorganic crystals inserted into the plastic mass are of nanoscale dimensions. Ideally, a composite scintillator would have an efficiency and resolution similar to those of an inorganic scintillator, while retaining the low cost and manufacturability of the organics [2].

These composites may be of a matrix type, where the functional fillers are mixed with a polymer matrix directly before the polymerisation process. Among others, the composites based on the polystyrene (PS) and polymethyl methacrylate (PMMA) are used for the fabrication of scintillators that can be used in particle detectors, radiation detectors, X-ray security, space technologies, nuclear cameras, solar and nuclear energetics, medicine, biology, and many other branches of the science and technology [3]. New composite scintillation detectors were reported to have high photoluminescence intensity and decay time in the nanosecond range. They were obtained by incorporation of PPO and o-POPOP organic scintillators into porous sol–gel silica matrices [4]. In the reported study on scintillators with pulse-shape discrimination capability, all PS samples also had the additions 0.1 wt% of 1,4-di-(2-(5-phenyloxazolil))-benzene (POPOP) as a wavelength shifter [5].

The present study is dedicated to the optical properties of the scintillators based on polystyrene related to the properties described in the International Standard ГОСТ 12736-86 and Ukrainian technical guide ТУ 6-09-38-82 on scintillators, as well as the guide ТУ 6-09-06-824-86 on fiber optics. PS is a transparent polymer of amorphous or non-crystalline structure with a glass-transition temperature $T_g = 100°C$, making it hard and brittle at room temperature [6]. It is a very clear material with good optical properties. PS does not exhibit a melting point, but it starts softening at temperatures of 80–85°C, and at 150°C, it becomes highly elastic [7]. The scintillator material under investigation in the present study was a luminophore o-POPOP non-matrix composite with a PS base. It was obtained by high-temperature polymerization for 30–50 hours, and subsequently underwent machining with cutting tools, then grinding and polishing. The main parameter for surface quality evaluation was *Ra*, which was expected to reach $Ra < 0.25$ μm.

According to the standards, the residual amount of monomer must not exceed 2%. The light output of scintillators must be no less than 80% of the standard ascribed to the specific dimensions, and, during the certain period of work, it must not drop more than 20% of the initially obtained value. The work period in a normal environment required by the standard is 48 months, which seems too short and even irrational. That is why the investigations were aimed to understanding the influence of the machining process, especially finishing procedure, on the durability of the scintillators.

1. Materials and methods

After polymerization, large sheets of the non-matrix composite of PS base with a luminophore o-POPOP ingredient were obtained, as shown in Fig. 1.

The polymer sheet was then cut into the samples for further research, leaving a 5–10 mm allowances for further machining. Dimensions of the samples were 800×400×40 and 800×400×60 mm. First, three series of samples were prepared for light output investigations, and each of them underwent the following machining:

1) Milling with tungsten carbide BK8, grinding, and polishing;
2) Milling with synthetic diamond CKM-P and grinding; and,
3) Micro-milling with natural diamond only.

To check the light output of the machined samples, the radiation source $^{90}S_r$ was used. It was placed in the central part of the examined sample whose back side was made black. Light output was measured with a photomultiplier.

For the investigations on the correlation between machining parameters and final roughness, another three

Fig. 1. Sheets of the non-matrix composite of PS base with luminophore o-POPOP ingredient obtained after polymerization at SCI "Monocrystals" Ukrainian National Academy of Science

series of samples were prepared. The choice of cutting tools was made based on the results of previous studies reported in [8] and [9]. Samples of each group were machined with the respective cutting tools made out of three different material types:

1) Refractory alloy BK8 (Russian nomenclature), which is built of a WC small size grain bounded by cobalt (8%), typically used for initial machining processes;
2) Synthetic polycrystalline diamond grains composite CKM-P (Russian nomenclature, see [10]); and,
3) Natural diamonds mined from the Earth.

The abovementioned series were divided into two groups each. The respective groups underwent machining with different feed rates, while the cutting depth was left unchanged, and with different cutting depths, while the feed rate remained unchanged. The cutting feed was varying from 0.01 to 0.15 mm/tooth, and the depth varied from 0.001 to 5 mm; however, in all experiments, the cutting speed remained the same at v = 1750 m/min.

Analysis of surface and the determination of roughness *Ra* were made with a Wyko RST-500 Optical Surface Profiler with PSI (phase-shifting interferometry) and VSI (vertical scanning interferometry) modes [11]. Interferometry systems, WYKO NT-2000 and WYKO NT-6000, based on a Mirau interference microscope were also used [12].

The visual analysis of the final surface quality was performed using a 3D microscope, МБС – 9 (Russian nomenclature), with 60× zoom. From the machined side, the photographs were made with a digital camera (Canon A300), which made the qualitative and quantitative evaluation of the edge chipped cracks available.

Finally, the research on optical durability was performed according to the International Standard ГОСТ 10667-90, using the methodology described in detail in [13]. Physically, the experiment means the immersion of the examined material in the reagent environment that accelerates its degradation. In the case of optical properties, the surface smoothness degradation accompanied by micro- and nano-cracks leads to the loss of transparency. Since the initial state of the surface with its asperities and edge chipped cracks caused by the machining inevitably determines further degradation processes, the investigations were to shed some light on the relation between the machining method and the durability of the optical properties.

During the experiments, the examined samples were immersed in heptane $H_3C(CH_2)_5CH_3$ at τ = 20 ±2° C. After a certain time in heptane, the surface and edges were inspected visually under the abovementioned microscope МБС – 9, and the light going through the specimen was measured at the distance of 40 cm.

3. Results and discussion

3.1. Impact of machining process on the light outlet

Analysis of the experimental results led to the conclusion that the diamond micro-milling was a sufficient process to obtain the required parameters of th light output of PS-based scintillators. Further grinding and polishing of the surfaces after diamond micro-milling did not improve the light output substantially.

Figures 2 and 3 present the results of light intensity measurements for the samples of 40 mm and 60 mm thicknesses, respectively.

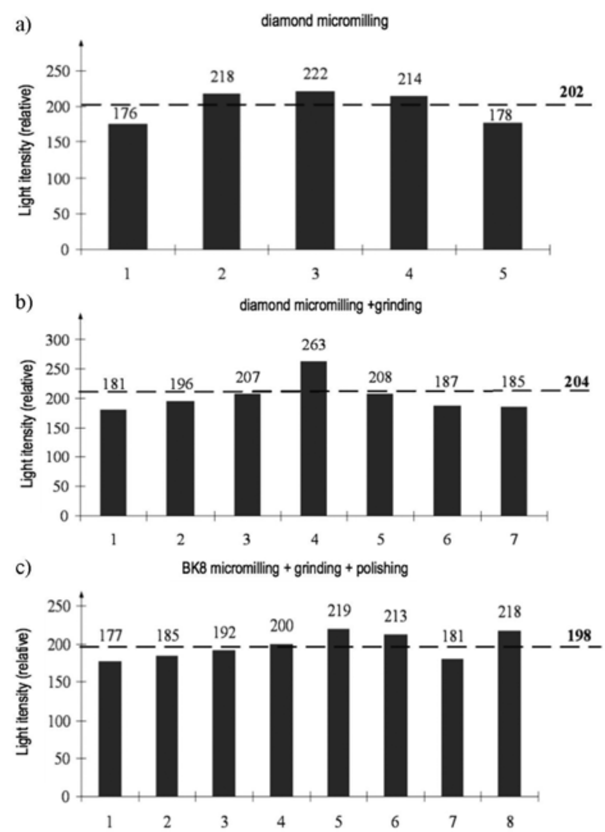

Fig. 2. Light output of the samples 800×400×40 mm after (a) milling with natural diamond, (b) milling with synthetic diamond CKM-P and grinding, (c) milling with tungsten carbide BK8, grinding and polishing

For the machined samples, the average light output remained essentially the same after grinding and polishing as achieved after diamond micro-milling. The samples of 40 mm thickness (Fig. 2) had an average relative light intensity of 202 units after milling, 204 after subsequent grinding, and 198 after polishing. Similarly, the samples 60 mm thick (Fig. 3), after the same machining operations, had a light intensity of 184, 185, and 179 units, respectively. The differences between the average values obtained after each subsequent operation was 6 units, which appeared to be far smaller than those

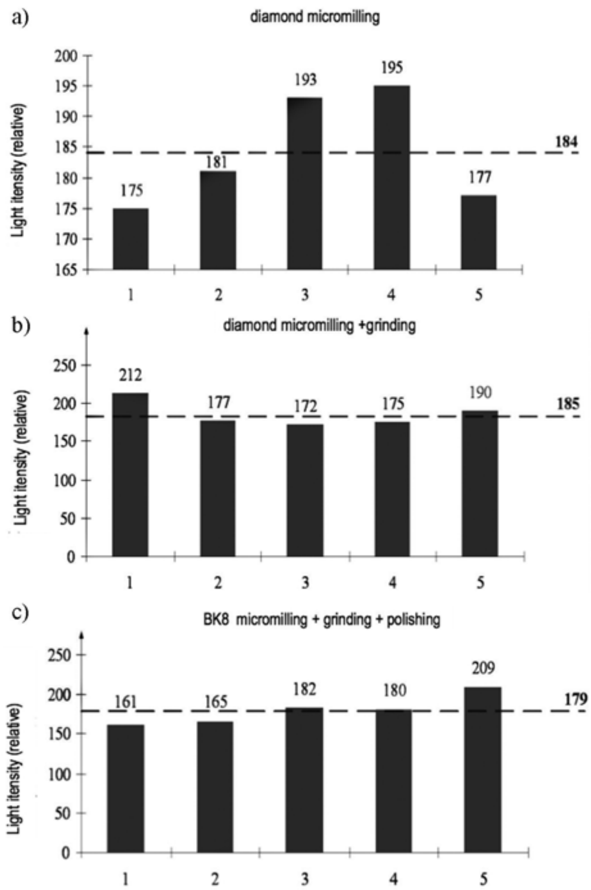

Fig. 3. Light output of the samples 800×400×60 mm after (a) milling with natural diamond, (b) milling with synthetic diamond CKM-P and grinding, (c) milling with tungsten carbide BK8, grinding and polishing

between the single samples after the same operations. For example, after micro-milling Sample 1 provided a light intensity of 175 units, while the Sample 4 had 195 units, so the difference was 20 units.

Inspection of the machined surfaces provided evidence that the surface temperature increase during the grinding process had a negative impact on the microscale topography and resulted in irregular asperities. In some cases, the outer layer worsened irreversibly, and further improvement of the optical properties became impossible. Then, it was assumed that the high hardness of abrasive material, compared with the grinded polymer hardness, in fact, introduced the mechanical microscale damages. Dimensions of those damages, however, were too large to remove with further polishing of those surfaces.

Similarly, it was observed that the local rise of surface temperature during the polishing process sometimes causes surface defects like scorches and melting zones. On the other hand, the diamond micro-milling was able to obtain the surface roughness of *Ra* = 0.04 – 0.08 μm, as presented below in the next section, which was extremely good result, especially as compared to *Ra* = 0.25 μm required by the Standard. A typical polishing operation is expected to ensure surface roughness *Ra* = 0.1 – 0.3 μm [14], which is not an improvement after *Ra* = 0.04 μm is obtained by the diamond micro-milling.

3.2. Impact of machining parameters on the surface roughness

It was found that the cutting feed could have a different impact on the examined material roughness, depending on the machining process stage. For example, rough milling with the tungsten carbide BK8 cutting tools provided an almost proportional increase of *Ra* related to the cutting feed increase. At the same time, the increase of the cutting depth had almost no influence on the resulting roughness, as seen in Figure 4. Here, the cutting depth was d = 1 mm when the feed was changed, and the cutting feed was f = 0.09 mm/tooth when the depth was changed. For all experiments, the cutting speed was the same (v = 1750 m/min), the cutting tool front angle was γ = 21°, and the main back angle was α = 21°.

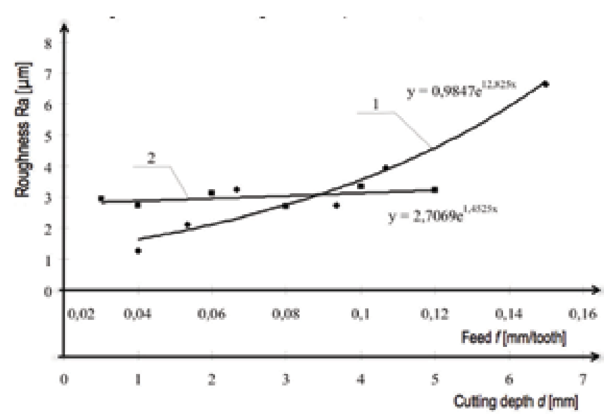

Fig. 4. Dependence of roughness *Ra* on the cutting feed *f* (Curve 1) and depth *d* (Curve 2) during the rough milling (WC cutting tool)

On the other hand, the relation between the roughness and cutting feed for the semi-finishing milling with the cutting tool CKM-P is not so simple. There is a range of cutting feeds from f_z = 0.03 up to 0.06 mm/tooth, when the roughness is minimal and lay below *Ra* = 0.6 μm. When the cutting feed is reduced below f_z = 0.03 mm/tooth, the rapid increase of *Ra* indicates the worsening of surface quality, as shown in Figure 5. Here, the cutting depth was d = 0.1 mm when the feed was changed, and the cutting feed was f = 0.047 mm/tooth when the depth was changed. For all experiments, the cutting speed was the same (v = 1750 m/min), the cutting tool front angle was γ = 4°, and the main back angle was α = 12°.

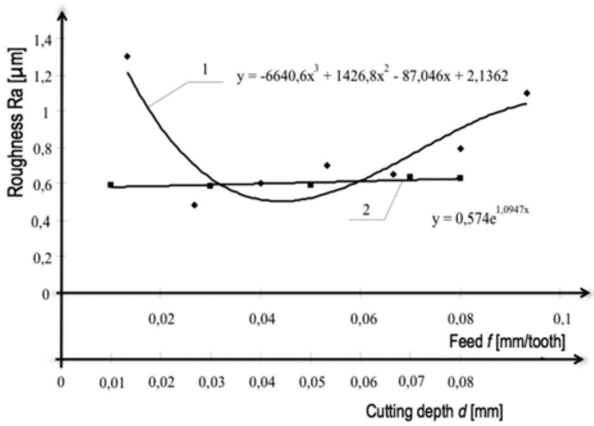

Fig. 5. Dependence of roughness *Ra* on the cutting feed *f* (Curve 1) and depth *d* (Curve 2) during the semi--finishing (synthetic diamond cutting tool)

Visual inspection of the surfaces obtained at the small cutting feeds like $f = 0.01$ mm/tooth, where the resulting roughness is very high, up to $Ra = 3$ µm, revealed that there are numerous burrs and melted zones. It can be explained when considering that the removed layer thickness was smaller than the radius of the cutting edge. As a result, the cutting tool was unable to cut into the material, so it was sliding on its surface without removing a chip. In these conditions, the small amounts of removed material were welded back into the surface layer, substantially worsening its quality.

On the other hand, at the cutting feeds $f_z = 0.03$ – 0.06 mm/tooth, the conditions in the machining zone were optimal. Namely, the shear cross-section is large enough, and the speed of the heat source related to the surface is decreased. As a result, the machined material is deformed to a smaller degree. However, a further increase of the cutting feeds above f_z inevitably results in worsened roughness caused by the kinematic factor.

Figure 6 presents the results obtained for the natural diamond micro-milling. Here, the cutting depth was $d = 0.05$ mm when the feed was changed, and the cutting feed was $f = 0.025$ mm/tooth when the depth was changed. For all experiments, the cutting speed was the same ($v = 1750$ m/min), the cutting tool front angle was $\gamma = 4°$, and the main back angle was $\alpha = 12°$.

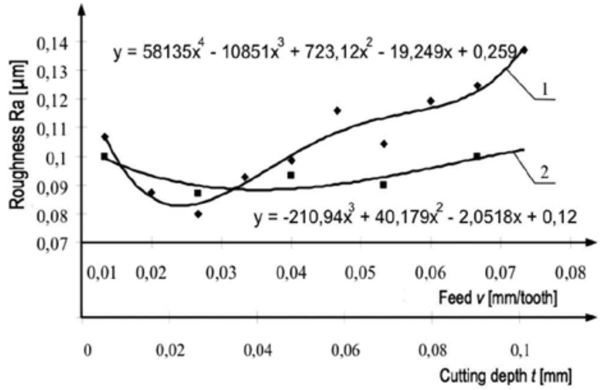

Fig. 6. Dependence of roughness *Ra* on the cutting feed *f* (Curve 1) and depth *d* (Curve 2) during the finishing (natural diamond cutting tool)

The shape of Curve 1 obtained for the natural diamond was quite like the one obtained for synthetic diamond composite cutting tool. General phenomena are similar as in the case of semi-finishing described above, but the roughness parameter *Ra* appears to be much smaller. The best results were obtained for optimal cutting feeds of $f_z = 0.02$ – 0.03 mm/tooth. Considerable worsening of *Ra* was observed when *f* was increased above f_z, and visual inspection revealed numerous burrs and melted zones.

In general, it can be stated that the surface quality of machined polystyrene is much less sensitive to the cutting depth changes than to the cutting feeds during the milling of any kind. In the case of natural diamond, the minimal roughness $Ra = 0.086$ – 0.090 µm was obtained for the cutting depth $d = 0.03$ – 0.07 mm. Other values of *d* provided an insufficient increase of the roughness *Ra*. In the case of rough milling, the increase of cutting depth from 1 up to 5 mm caused the increase of *Ra* just for 0.4 µm, which corresponded with 20% of its value.

An example of the roughness measurement after diamond micro-milling is presented in Figure 7a. *Ra* obtained in the *x*-axis was 119 nm, and it was 55 nm in the y-axis, which gave an overall $Ra = 115$ nm. Despite the distinguishably directed surface topography after the milling, the surface prevented a high degree of integrity with nanoscale asperities, which provided its high optical properties.

Interestingly, the specimen after natural diamond micro-milling (Fig. 7b) did not improve its transparency after superfinishing. In spite of reducing the roughness *Ra* below 2 nm and the minimization of directed cutting edge paths, the surface looked somewhat matt instead of the expected shiny surface. Nevertheless, its transparency was neither affected nor improved.

The obtained results enabled us to determine optimal milling parameters for PS scintillators, making it possible to obtain high quality surfaces that ensure the required optical properties of PS-based scintillators.

3.3. Edge formations under different machining parameters

The issue of edge formations dependent on the machining parameters was not addressed properly. In industrial practice, it is commonly believed that the final polishing removes most of the microcracks and smooths the chipped edges. However, even after the polishing, optical surfaces have microcracks that initiate the degradation process during exploitation. Similarly, the degradation process easily starts along the edges

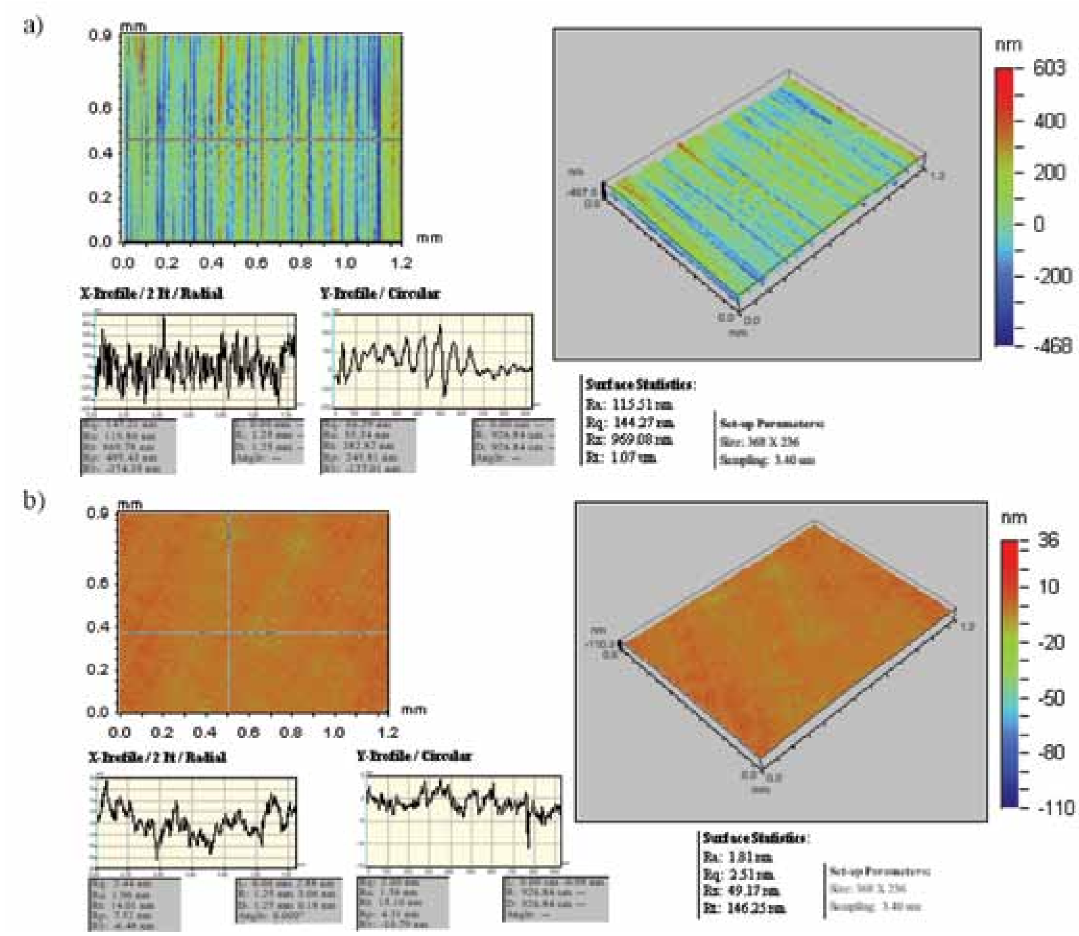

Fig. 7. Example of topography analysis of a PS optical composite specimen: (a) after natural diamond micro-milling only, (b) after micro-milling and superfinishing

where some material is chipped off (burr), even after the surface is smoothed by polishing. Residual surface porosity enables the atmospheric oxygen to diffuse into the material, while the material chipped off during the milling leaves certain inner stresses that are not removed by polishing and provoke crack propagation later on. The surface microscale cracks need not be too numerous to reduce the optical properties of the material substantially.

Dimensions of edges microcracks left by the chipped off material depend on many factors and machining parameters. For instance, Figure 8 presents an example of the PS scintillator edges after synthetic diamond face milling at a cutting depth d = 0.1 mm, feed f = 0.026 mm/tooth, and speed v = 1750 m/min. Dimensions of the micro-damages are almost 3 times larger at the cutter exit side (exit burr, Fig 8b) than at the entrance side (entrance burr, Fig. 8a).

a) b)

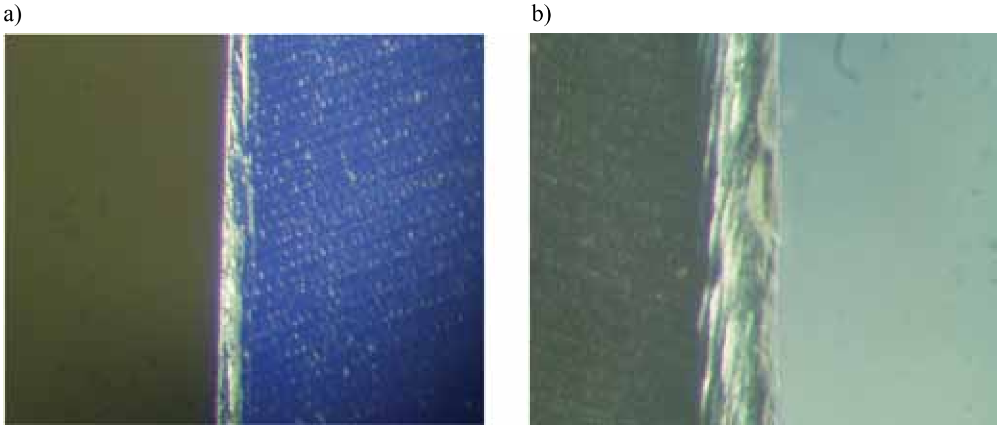

Fig. 8. Edge micro-damages after CKM-P face milling: a) entrance burr, b) exit burr

During the rough milling with WC cutting tool (BK8), the dimensions of the burr grow almost proportionally with the increase of cutting feed. In some cases, the burr dimensions are larger than the allowances for semi-finishing and finishing, which are usually 0.15 – 0.6 mm, so no subsequent machining is able to recover the damaged edges. Figures 9–13 present the graphs of the burr dimensions versus cutting depth and feed, respectively, in various milling conditions.

Figure 10 (tungsten carbide BK8 cutting tool) indicates that the increased cutting depth up to 5 mm caused edge damages (exit burr) as big as 0.75 mm. Entrance burr creation also takes place, but its dimensions are much smaller.

The synthetic diamond semi-finishing provided smaller edge damages than tungsten carbide rough milling, while the general trend remained the same, as seen in Figures 11 and 12. Perhaps it was so because of better heat removal from the cutting area, as well as smaller cutting edge diameter resulting in better chips formation. Visual inspection of the damaged edges led to the conclusion that the entrance burr is a result of material squeezing, and the damages chipped out are fewer. The layers of polymer material that underwent densification are clearly distinguishable.

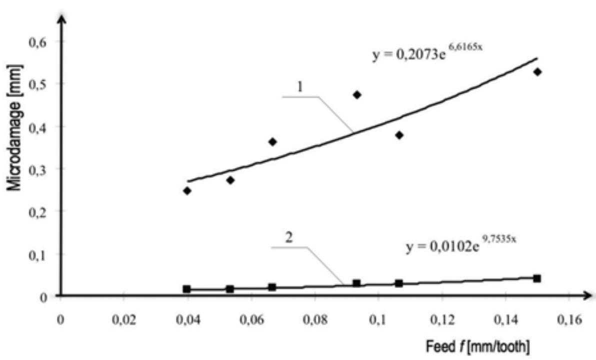

Fig. 9. Edge micro-damages after BK8 face milling: 1 – exit burr, 2 – entrance burr (d = 1 mm, v = 1750 m/min, γ = 21°, α = 21°)

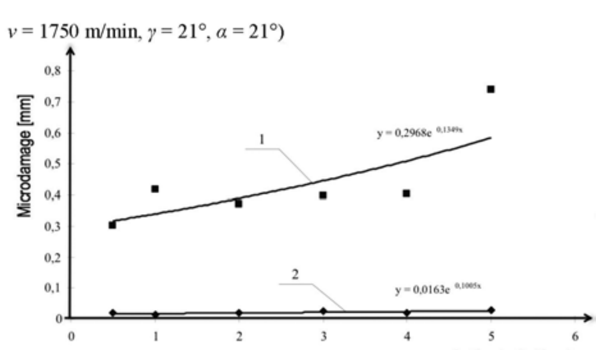

Fig. 10. Edge micro-damages after BK8 face milling: 1 – exit burr, 2 – entrance burr (f = 0.09 mm/tooth, v = 1750 m/min, γ = 21°, α = 21°)

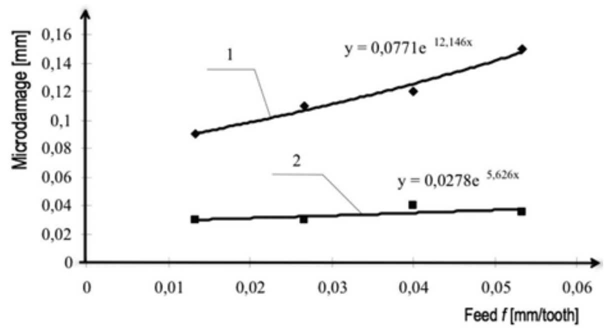

Fig. 11. Edge micro-damages after CKM-P face milling: 1 – exit burr, 2 – entrance burr (d = 0.1 mm, v = 1750 m/min, γ = 4°, α = 12°)

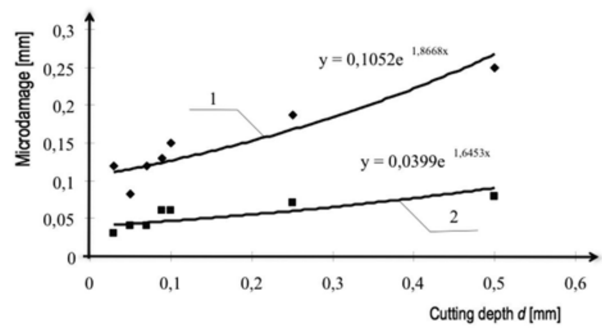

Fig. 12. Edge micro-damages after CKM-P face milling: 1 – exit burr, 2 – entrance burr (f = 0.047 mm/tooth, v = 1750 m/min, γ = 4°, α = 12°)

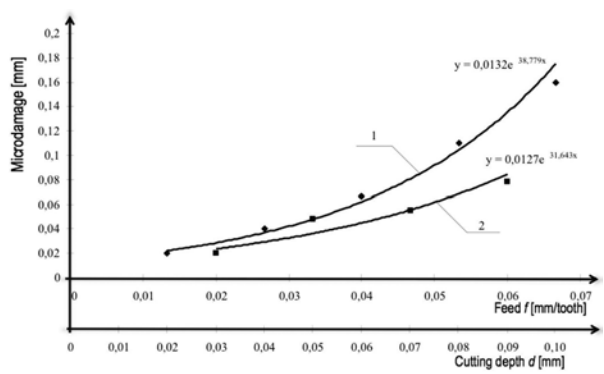

Fig. 13. Edge micro-damages (exit burr) after natural diamond face milling: 1 – dependent on cutting feed at depth d = 0.05 mm, 2 – dependent on depth at cutting feed f = 0.025 mm/tooth (v = 1750 m/min, γ = 4°, α = 12°)

Finishing micro-milling with the natural diamond cutters resulted in no entrance burrs, so Figure 13 presents only exit burrs. The machined edge was found to be rounded instead, with the radius below 0.01 mm. The graphs in Figure 13 indicate that the dimensions of micro-damages increase with the increase of both cutting feed and depth. The minimized edge damage can be explained considering the fact that the natural diamond cutting tools meet all of the requirements of the machining of polymer optical surfaces. Namely, it has a minimal radius of the cutting edges, minimal roughness of the working surfaces, high heat conductivity and capacity, high wear resistance, and minimal friction and minimal adhesion between the tool and machined material.

3.4. Durability of optical properties

The trial of machined specimens in heptane provided interesting results. A clear correlation between the machining conditions and the durability was observed, and it was substantially influenced by the edge micro-damages. Thus, three areas of the machined optical surface were distinguished, as shown in Figure 14:

1) The edge area where parts of material were chipped out;
2) The transitional area with microcracks caused by the material chipped out from the edge; and,
3) The machined surface with its own asperities, not affected by the edge micro-damages.

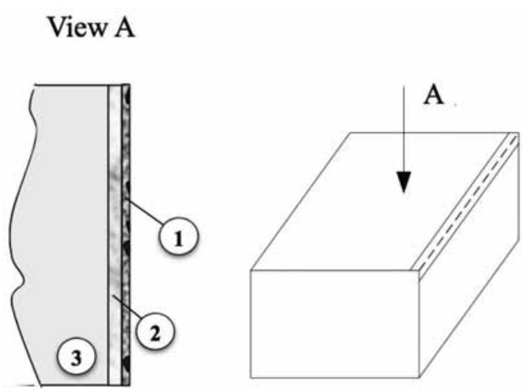

Fig. 14. Machined surface affected by the edge micro-damages (explanations in text)

Surfaces of all the specimens milled with tungsten carbide BK8 cutting tools at the cutting depth $d = 1$ mm and a feed $f = 0.05 – 0.15$ mm/tooth after a 20 minutes trial in heptane reveal deep single microcracks, as well as "whitish" areas up to 2 cm large. The samples machined at cutting depth $d > 1$ mm lost their transparency almost completely. Their surfaces were matt, and the number of microcracks was as high as 60 per mm^2.

The specimens machined with composite synthetic diamond CKM-P looked much better after the heptane trial. They had, however, a grid of microcracks on the entire surface, and deep long cracks along the edges in Area 2 (Fig. 14), obviously generated by the exit burr. Some of those cracks were of 7 mm long and 1 μm wide.

The natural diamond micro-milling, as expected, revealed the best results, but the obtained values exceeded all the expectations. On the surface of samples milled at cutting feed $f = 0.03$ mm/tooth and depth $d = 0.03$ mm, microcracks appeared only after 45 minutes, and their dimensions were approximately 1 mm in length and 0.5 μm in width. It is assumed that the durability of 45 minutes in heptane corresponds with approximately 10 years of exploitation in normal conditions [15]. Such a long durability, which is almost three times longer than prescribed in the Standard, can be attributed to only proper machining conditions, because all other material parameters of the specimens were the same.

It is widely known that "the type of materials used is important, but the functionality of the material expected by the user is crucial" and that many attempts are made in order to increase the operational durability [16]. The abovementioned machining parameters ensure a high level of surface integrity that provided high durability of optical properties. Other researchers reported the influence of machining parameters on the surface integrity of hard machined materials in terms of crack propagation dependent on feed rate [17], temperature in the cutting zone [18], inner residual stresses and roughness [19], and subsurface damages induced by grinding [20]. The results discussed above provided direct evidence of the high optical durability of scintillator dependent on the surface integrity.

Conclusions

The described research results enabled us to evaluate qualitatively and quantitatively relations between the machining conditions and surface quality as well as the optical properties of PS-based composite scintillators with o-POPOP addition. It is recommended to perform the rough milling at a cutting feed no higher than $f = 0.1$ mm/tooth. Moreover, the optimal semi-finishing and finishing milling parameters correspond with $f_z = 0.02 – 0.04$ mm/tooth, while both larger and smaller feed values rather worsen the machined surface quality.

As for the cutting depth, it was found that the better results could be achieved at $d = 2 – 5$ mm for rough milling with a tungsten carbide BK8 tool ($d = 0.1 – 0.7$ mm) for semi-finishing milling with a composite synthetic diamond tool, and $d = 0.03 – 0.07$ mm for finishing micro-milling with a natural diamond cutter. In some cases, the range of those parameters may be widened after the surface quality requirements are agreed with the customer.

Analysis of edge damages (entrance and exit burr) enabled finding out the relations between the machining parameters and the dimensions of micro-damages. The most important, however, was finding the correlation between surface and edge quality and the durability of optical properties. Certain parameters of natural diamond micro-milling provided such a high quality of surface and edges that the durability of their optical properties extended up to 45 minutes in heptane, which corresponded with 10 years in normal exploitation conditions.

Evidently, the obtained durability is due to the high level of surface integrity with an optimized temperature in the cutting zone, as well as minimized microcracks, edge micro-damages, and inner stresses.

Acknowledgements

The article is the detailed and full version of the paper originally presented at the conference 8th Symposium on Composites and Layer Constructions, Wroclaw/Poland, 26–29 October 2017, with an extended abstract published in Proceedings, pp. 31–32. Authors express their sincere gratitude to SCI "Monocrystals" Ukrainian National Academy of Science for the polystyrene composite materials delivered for the researches, and to Optical Science Lab., University College London, and IFQ, Otto-von-Guericke University Magdeburg, for cooperation in surface measurements.

Funding sources

This research did not receive any specific grant from funding agencies in the public, commercial, or not-for-profit sectors.

References

1. Birks J.B.: *The Theory and Practice of Scintillation Counting*. Oxford: Pergamon Press, 1964.
2. Smith A.Li.N., Hehlen M.P., McKigney E.A., Gardner R.: Light yield measurement method for milled nanosize inorganic crystals. *Applied Radiation and Isotopes*, 2012, 70(7), pp. 1219–1222. DOI: 10.1016/j.apradiso.2011.09.021
3. Globus M.E., Grinev B.V.: *Inorganic Scintillators: New and Traditional Materials*. Kharkov: Acta, 2000 (in Russian).
4. Viagin O., Masalov A., Bespalova I., Zelenskaya O., Tarasov V., Seminko V., Voloshina L., Zorenko Yu., Malyukin Yu.: Luminescent properties of composite scintillators based on PPO and o-POPOP doped SiO_2 xerogel matrices. *Journal of Luminescence*, 2016, 179, pp. 178–182. DOI: 10.1016/j.jlumin.2016.07.001
5. Zhmurin P.N., Lebedev V.N., Titskaya V.D., Adadurov A.F., Elyseev D.A., Pereymak V.N.: Polystyrene-based scintillator with pulse-shape discrimination capability. *Nuclear Instruments and Methods in Physics Research A*, 2014, 761, pp. 92–98. DOI: 10.1016/j.nima.2014.05.084
6. Ibeh C.C.: *Thermoplastic Materials: Properties, Manufacturing Methods, and Applications*. Boca Raton: CRC Press, 2011.
7. Sahno T.V., Barashkov N.N., Kraynov I.P.: *Organic materials for luminescent sunlight concentrators*. Moscow: NIITECHIM, 1992 (in Russian).
8. Grabchenko A.I., Verezub N.V., Lavrinenko S.N., Fererov A.M., Getmanov A.A., Horvath M., Mamalis A.G.: Precision Machining of Optical Products Made from Polymeric Materials. *The International Journal of Advanced Manufacturing Technology*, 2001, 17(2), pp. 93–103. DOI: 10.1007/s001700170
9. Mamalis A.G., Lavrynenko S.N.: On the precision single-point diamond machining of polymeric materials. *Journal of Materials Processing Technology*, 2007, 181(1–3), pp. 203–205. DOI: 10.1016/j.jmatprotec.2006.03.060
10. Petrushin S.I., Danilenko B.D., Retiunsky O.Yu.: *Optimization of the materials properties in the composite cutting edge of the cutting tools*. Tomsk: Tomsk Technical University, 1999 (in Russian).
11. Mathia T.G., Pawlus P., Wieczorowski M.: Recent trends in surface metrology. *Wear*, 2011, 271, pp. 494–508. DOI: 10.1016/j.wear.2010.06.001
12. de Groot P.J.: *Interference Microscopy for Surface Structure Analysis*. In: Yoshizawa T. (Ed.): *Handbook of Optical Metrology: Principles and Applications*. Boca Raton: CRC Press, 2015, pp. 791–828.
13. Narisawa I.: *Resistance of Polymer Materials*. Moscow: Chemistry, 1987 (in Russian).
14. Grzesik W.: Effect of the machine parts surface topography features on the machine service. *Mechanik*, 2015, 8–9, pp. 587–593 (in Polish). DOI: 10.17814/mechanik.2015.8–9.493
15. Borisenko A.Yu., Senchishin V.G., Lebedev V.N.: Long-term stability of the polystyrene scintillators. *Visnyk of Kharkov University: Physics*, 1998, 421, pp. 33–36.
16. Mizak W., Mazurkiewicz A.: System for nonstandard testing of erosive wear of materials. *Journal of Machine Construction and Maintenance*, 2017, 4, pp. 27–35.
17. Choi Y.: Influence of feed rate on surface integrity and fatigue performance of machined surfaces. *International Journal of Fatigue*, 2015, 78, pp. 46–52. DOI: 10.1016/j.ijfatigue.2015.03.028
18. Klocke F., Gierlings S., Brockmann M., Veselovac D.: Influence of Temperature on Surface Integrity for Typical Machining Processes in Aero Engine Manufacture. *Procedia Engineering*, 2011, 19, pp. 203–208. DOI: 10.1016/j.proeng.2011.11.102
19. Jawahir I.S., Brinksmeier E., M'Saoubi R., Aspinwall D.K., Outeiro J.C., Meyerb D., Umbrello D., Jayal A.D.: Surface integrity in material removal processes: Recent advances. *CIRP Annals – Manufacturing Technology*, 2011, 60(2), pp. 603–626. DOI: 10.1016/j.cirp.2011.05.002
20. Zhao Y.J., Yan Y.H., Song K.Ch., Li H.N.: Robust and automatic measurement of grinding-induced subsurface damage in optical glass K9 based on digital image processing. *Archives of Civil and Mechanical Engineering*, 2018, 18(1), pp. 320–330. DOI: 10.1016/j.acme.2017.07.009